Research correspondence

Optimising the method for visualising mouse meibomian gland using eyelid whole-mount lipid staining

Yuki Hamada[1†], Lena Sasaki[1†], Hikari Uehara[1], Tomo Suzuki[2,3], Shigeru Kinoshita[4], Kento Otsuka[5], Akio Kihara[5], Yoshiaki Yamaguchi[1], Takahito Miyake[1], Masao Doi[1,*]

[1]Department of Systems Biology, Graduate School of Pharmaceutical Sciences, Kyoto University, Sakyō-ku, Kyoto, Japan
[2]Department of Ophthalmology, Kyoto Prefectural University of Medicine, Kamigyō-ku, Kyoto, Japan
[3]Department of Ophthalmology, Kyoto City Hospital, Nakagyō-ku Kyoto, Japan
[4]Department of Frontier Medical Science and Technology for Ophthalmology, Kyoto Prefectural University of Medicine, Kamigyō-ku, Kyoto, Japan
[5]Laboratory of Biochemistry, Faculty of Pharmaceutical Sciences, Hokkaido University, Kita-ku, Sapporo, Japan

[†]Y.H, and L.S. contributed equally to this work.

[*]Address correspondence to:
Masao Doi, doimasao@pharm.kyoto-u.ac.jp

Keywords: Meibomian gland, Whole-mount staining, Pigment bleaching

Black opaque pigment residing in the eyelids of C57BL/6 inbred mice and other related mice hampers detailed whole-mount macroscopic observation of the meibomian gland [1, 2]. Owing to this inherent problem, studying mouse meibomian gland histology is and has been mainly performed by standard tissue-sectioning method, which allows detection of cross-sectioned image of the meibomian gland without significant interference from the interstitial pigments. However, appearance of tissue section of the meibomian gland is variable between sections. The chief advantage of whole-mount histological analysis, in comparison, is that it enables examination of the whole structure of the meibomian glands, not sections thereof, allowing accurate (non-section-biased) quantitative investigation of their morphology. In the present study, we optimized the method for visualizing mouse meibomian gland using eyelid whole-mount lipid staining. We prepared bleached eyelid samples and made them transparent. By doing so, we visualized the entire meibomian gland structure across the eyelid (see Fig. 1).

As a basic design for improvement of meibomian gland staining, we have introduced pigment bleaching procedure, in which the eyelid tissues were treated with hydrogen peroxide (H_2O_2, Fig. 1A). The specimens were fixed prior to and after this treatment to minimize deformation. Thereafter, the bleached fixed tissues were subjected to colorimetric lipid staining, followed by tissue clearing [3]. A modified aqueous-based tissue clearing method that does not contain delipidation was adopted, to preserve stained lipids in the meibomian gland. The details of our revised protocol and examples of its application are provided below.

First of all, we used C57BL/6 mice for the protocol; albino mice (such as BALB/c) may be an alternative mouse model to avoid pigment problem [1]. The skin around the eye, containing upper and lower eyelids, was excised as a whole tissue [3]. After fixation in a fixative buffer containing 4% (w/v) paraformaldehyde and 1% (w/v) glutaraldehyde in phosphate-buffered saline (PBS) for 24 h at 4 °C, the specimen was washed with PBS and bleached in 3% (v/v) hydrogen peroxide at 37 °C for 24 h. The specimen was subsequently post-fixed with 4%

paraformaldehyde-1% glutaraldehyde in PBS for 24 h and immersed into 50% ethanol for 10 min and 70% ethanol for 20 min. Then, lipid staining was performed as described [3]. In brief, the specimen was dipped in Sudan IV (Nacalai Tesque Inc)-saturated 70% ethanol solution containing 2% NaOH for 24 h with gentle rotation at room temperature (NaOH was included primarily for tissue maceration, while it also helps reduce pigments). Following extensive washes with 70% ethanol, the specimens were cleared by incubation with 25% *N*, *N*, *N*', *N*'-Tetrakis-(2-hydroxypropyl) ethylenediamine (Tokyo Chemical Industry) in glycerol overnight. Before being mounted in glycerin jelly, the lateral canthi of the eyes were cut open to make the specimens flat, and adhering connective tissues and debris were removed. Images of whole-mount meibomian glands were taken under a light-field microscope and analyzed using ImageJ (https://imagej.nih.gov/ij/). To see the potential improvement caused by pigment bleaching, we also prepared a sample treated in the same way as described above except omission of hydrogen peroxide treatment.

We observed that without hydrogen peroxide treatment, residual pigments, which changed in color (slightly brownish), remained around the orifice of the meibomian glands in upper and lower eyelids (Fig. 1B, arrows in (−) bleaching). Bleached samples, on the other hand, allow clear visualization of the entire meibomian gland structures (see Fig. 1B, (+) bleaching): Each single meibomian gland is composed of multiple acini connected via short ductules to a long central duct that extends to the meibomian gland orifice at the eyelid margin. These separate glands are arranged in parallel in a single row throughout the eyelid from the nasal to temporal edges, in both upper and lower eyelids. These structural features of the meibomian glands can be similarly identified in humans, as reported previously in depth [4, 5], indicating the fundamental anatomical similarity between human and mouse meibomian glands [2, 6]. Apart from the similarity, we found in mice several unique features, including a tuft of meibomian glands situated in the nasal corner and a relatively enlarged meibomian gland situated in the temporal

extremity in both upper and lower eyelids, illustrating the species difference in anatomy.

Using this modified method, we visualized age-associated meibomian gland morphological changes, using 18 month-old (mo) mice (Fig. 1C). The area of the meibomian gland, which can be measured without obstructions of pigments, was expectedly diminished by aging (18-mo vs 2-mo mice, $P < 0.01$, unpaired *t*-test). Because in this analysis photographs were binarized and quantified for colored lipid area, depletion of remaining pigment facilitates assessing Sudan IV stained area. In addition, structural changes, characterized by tubular thinning and shortening, and gland dropout, were also reportedly observed in aged mice, in a whole-mount view (Fig. 1C). These changes in size and structure were similarly observed in aged human meibomian gland [4, 5]; thus, age-associated tissue atrophy of the meibomian gland appears to be a common feature conserved between humans and mice as suggested [6].

As an exemplar application of our method to a mouse model showing structural abnormality of the meibomian gland, we used the fatty acyl-CoA reductase 2 (FAR2) knockout mice [7], which exhibit significant dilation of the central duct near the orifice of the meibomian gland, an observation made by conventional tissue sectioning method [7]. This marked structural alteration was reproducibly and clearly observed in our method (Fig. 1D). In addition, we also noted, through our method, that *Far2* knockout mice exhibit significant reduction in size of acini (Fig. 1D) linking the central duct, a structural phenotype that escaped notice in previous section-based phenotype analysis, suggesting the potential merit of non-biased whole-mount method examination. It has been biochemically reported that the melting point of the meibum lipids in the mice lacking the enzyme FAR2 is significantly higher (49°C) than in wildtype mice (37°C) [7]. Therefore, the meibum lipids in the *Far2* knockout mice do not melt at body temperature, resulting in plugging of the meibomian orifices [7]. The shrinking of linked acini may be a result of reduced production of lipid due to plugging or FAR2 deficiency.

In summary, we present evidence that pigment bleaching by hydrogen peroxide treatment

allows easier detection of whole-mount morphology and histo(patho)logy of the meibomian gland for C57BL/6 mice. H_2O_2 bleaching cleared pigmentation at the lid margin area; this will be of help in characterizing morphology at the terminal end of the duct (e.g., ductal dilation and/or obstruction at orifice) in a whole-mount view. Our visualizing method, combined with pharmacological and intersectional genetic approaches in mice [2], may facilitate further investigations into the mechanisms of the meibomian gland dysfunction and its associated ocular surface impairment.

Sources of support

This work was supported in part by research grants from the Ministry of Education, Culture, Sports, Science and Technology of Japan (22H04987, 22H00441, 20H05783, 20K21426), the Kobayashi Foundation, and the Kusunoki 125 of Kyoto University 125th Anniversary Fund.

Competing interests

The authors declare no competing interests.

References

[1] Mizoguchi S, Iwanishi H, Kokado M, Sumioka T, Parfitt GJ, Xie Y, et al. Ocular surface alkali injury damages meibomian glands in mice. Ocul Surf. 2017;15:713-22.

[2] Sun M, Moreno IY, Dang M, Coulson-Thomas VJ. Meibomian Gland Dysfunction: What Have Animal Models Taught Us? Int J Mol Sci. 2020;21:8822.

[3] Sasaki L, Hamada Y, Yarimizu D, Suzuki T, Nakamura H, Shimada A, et al. Intracrine activity involving NAD-dependent circadian steroidogenic activity governs age-associated meibomian gland dysfunction. Nat Aging. 2022;2:105-14.

[4] Knop E, Knop N, Millar T, Obata H, Sullivan DA. The international workshop on meibomian gland dysfunction: report of the subcommittee on anatomy, physiology, and pathophysiology of the meibomian gland. Invest Ophthalmol Vis Sci. 2011;52:1938-78.

[5] Obata H. Anatomy and histopathology of human meibomian gland. Cornea. 2002;21:S70-4.

[6] Nien CJ, Paugh JR, Massei S, Wahlert AJ, Kao WW, Jester JV. Age-related changes in the meibomian gland. Exp Eye Res. 2009;89:1021-7.

[7] Otsuka K, Sawai-Ogawa M, Kihara A. Formation of fatty alcohols-components of meibum lipids-by the fatty acyl-CoA reductase FAR2 is essential for dry eye prevention. Faseb J. 2022;36:e22216.

Figure Legend

Fig. 1. Improved visualization of the mouse meibomian glands by pigment bleaching. (A) C57BL/6 mouse eyelid before and after H_2O_2 treatment. (B) Outline of meibomian gland lipid staining. Pictures represent whole-mount mouse eyelids with or without H_2O_2 treatment. Arrows, black pigments remaining on the untreated eyelid. Box, high magnification view of meibomian gland in the bleached eyelid. (C) Atrophy of meibomian gland in aged mice. Group data show quantification of meibomian gland area of young (2 months) and aged (18 months) mice (n = 4 per group). Photographs were binarized and quantified for lipid area using ImageJ. Values represent the sum of the upper and lower eyelid glands. $^{**}P < 0.01$, t-test. Arrows, areas of gland loss. (D) Morphology of the meibomian gland in *Far2*$^{-/-}$ mice. Group data show quantification of mean width of the meibomian gland central ducts of upper eyelids (n = 3 per genotype) (*left*) and mean total size of linked acini of upper and lower eyelid meibomian glands in WT and *Far2*$^{-/-}$ mice (n = 3 per genotype) (*right*). The width was measured 200 μm from the eyelid edge. $^{**}P < 0.01$, $^{*}P < 0.05$, t-test. All values are presented as the mean ± SEM. mo, months old.

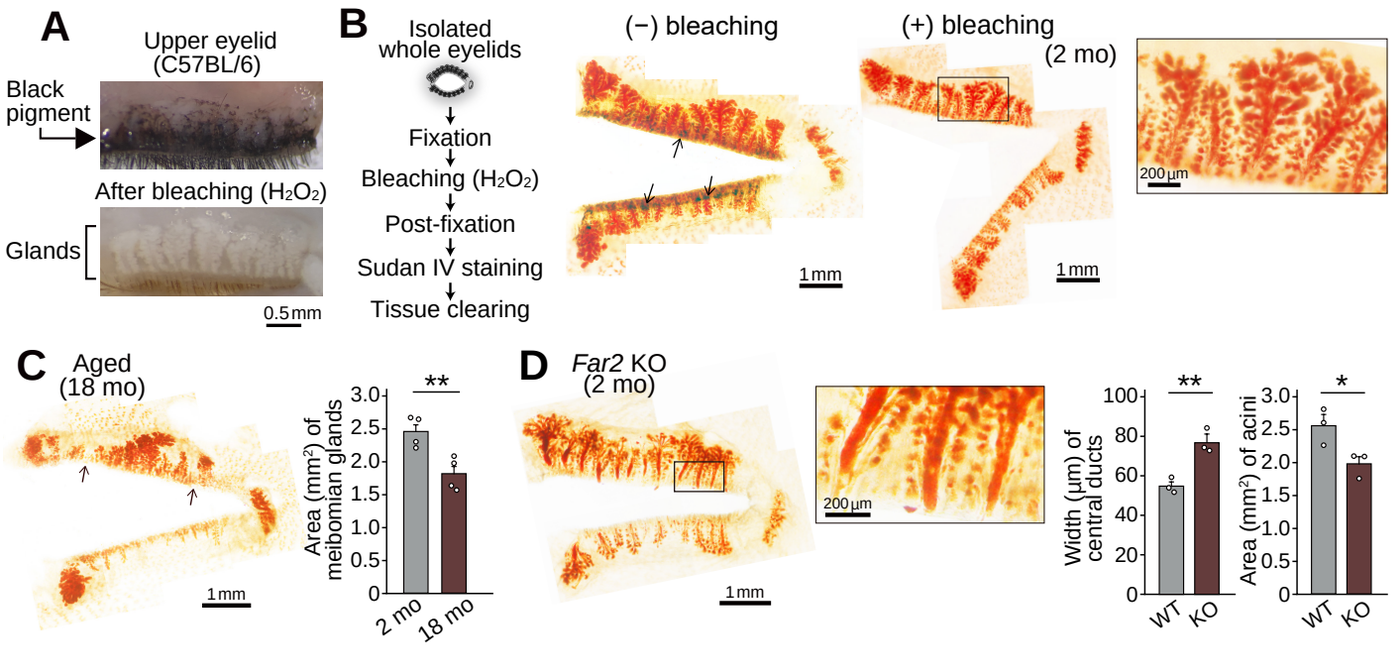
A
Upper eyelid
(C57BL/6)
Black
pigment
After bleaching (H2O2)
Glands
0.5 mm
B
Isolated
whole eyelids
Fixation
Bleaching (H2O2)
Post-fixation
Sudan IV staining
Tissue clearing
(−) bleaching
(+) bleaching
(2 mo)
1 mm
1 mm
200 µm
C
Aged
(18 mo)
1 mm
Area (mm2) of
meibomian glands
**
2 mo
18 mo
D
Far2 KO
(2 mo)
1 mm
200 µm
Width (µm) of
central ducts
**
WT
KO
Area (mm2) of acini
*
WT
KO

Figure 1